WESC 2023
23 - 26 MAY | GLASGOW, UK

WIND TURBINE ROTOR BLADE DEFORMATION RECONSTRUCTION USING SHAPE SENSING TECHNIQUES ON QUASI-CONTINUOUS OPTICAL FIBERS AND DISCRETE FBGS

Wind turbine rotor blade deformation reconstruction using shape sensing techniques on quasi-continuous optical fibers and discrete FBGs

Mini Symposia 6.2:

German research wind farm WiValdi – innovative instrumentation and advanced testing to enable a digital twin wind farm

DLR

Janto GUNDLACH, DLR - Institute of Aeroelasticity, Glasgow, 2023-05-23

Wind turbine rotor blade deformation reconstruction using shape sensing techniques on quasi-continuous optical fibers and discrete FBGs

Content

https://youtu.be/dRht4tkQJIM

Background and Motiviation

Origination of Shape Sensing

- crash of Helios due to pitch oscillations (2003)
- development of strain-to-deflection algorithms for wing structures
- real-time deflections from surface strains

Ko et al., 2007

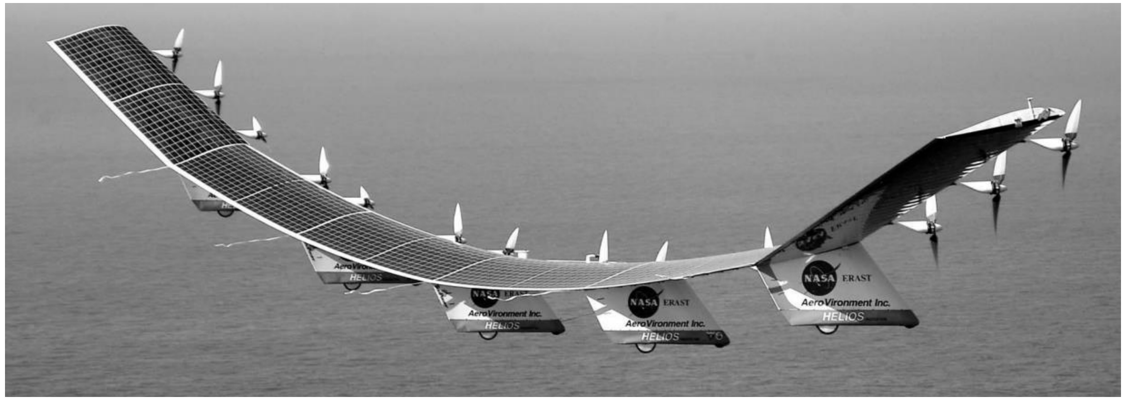

Potentials for research wind farm

- online-monitoring of modal parameters such as blade displacement mode shapes
- track rotor blade deflection over rotations, changing operational and environmental conditions
- more precise load assessment during operation

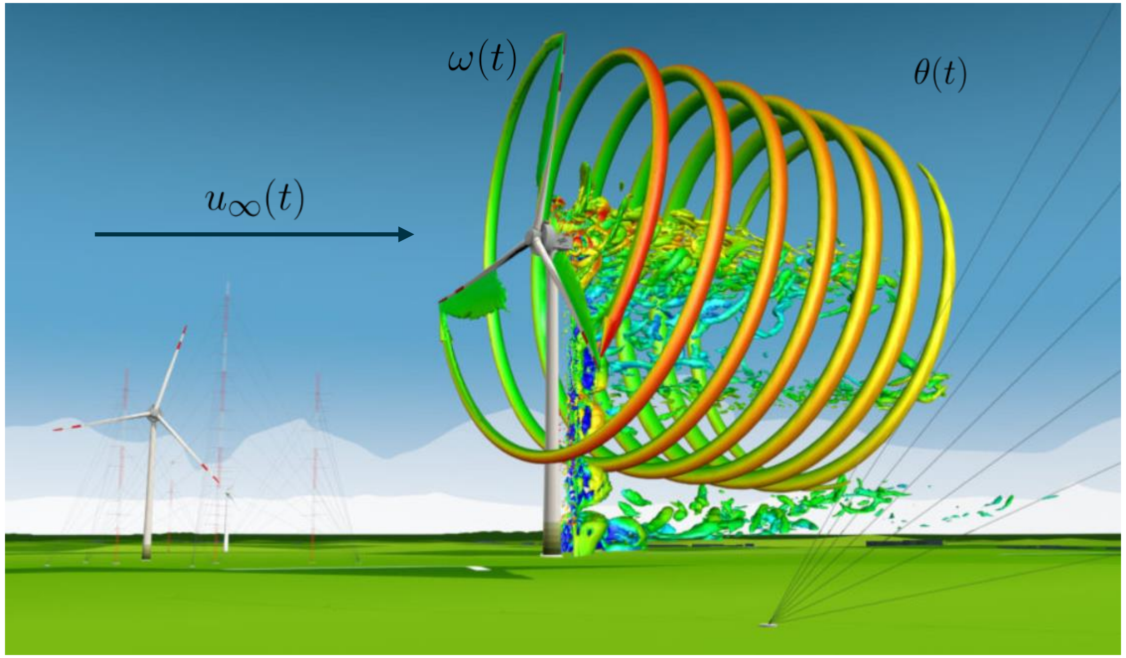

Test Scenarios in IWES Hall

Modal testing

- characterize modal parameters
- obtain data usable for Shape Sensing

Static load tests

- deflection reconstruction using internal strain instrumentation
- validation of estimates with measured deflection

Ko‘s Displacement Theory

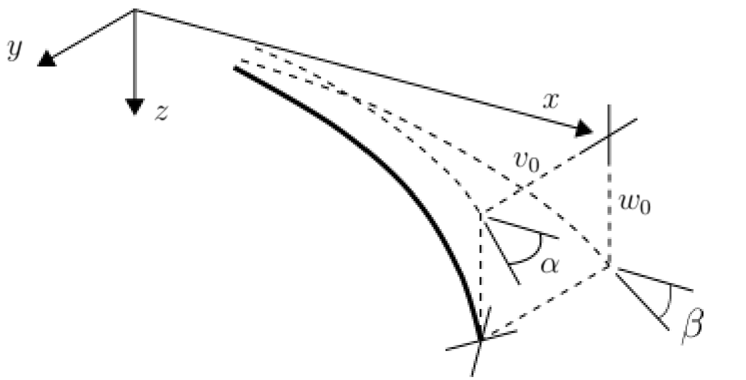

Assumptions

- Euler-Bernoulli kinematics
- plane systems
- no product moment of area
- no axial forces

Surface strain

$$\varepsilon_c = \frac{M_y c}{EI_{yy}} \Leftrightarrow w'' = -\frac{\varepsilon_c}{c}$$

$c:$ distance to neutral axis

Ko‘s approach

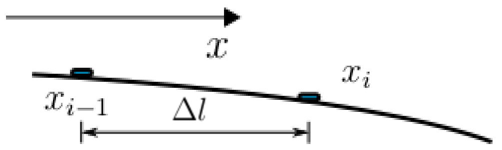

$$\Delta l = x_i - x_{i-1}$$

- equidistant spacing between ‘strain stations’
- piecewise linear bending moment and strain

$$\varepsilon(x) = \varepsilon_{i-1} - (\varepsilon_{i-1} - \varepsilon_i)\frac{x - x_{i-1}}{\Delta l}$$

- piecewise linear tapering

$$c(x) = c_{i-1} - (c_{i-1} - c_i)\frac{x - x_{i-1}}{\Delta l}$$

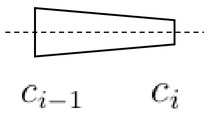

Slope and deflection equation

$$\tan\beta(x) = \int_{x_{i-1}}^{x} w''\mathrm{d}x + \tan\beta_{i-1}$$

$$w(x) = \int_{x_{i-1}}^{x} \tan\beta(x)\mathrm{d}x + w_{i-1}$$

$$\tan\beta_i = -\Delta l\left(\frac{\varepsilon_{i-1}+\varepsilon_i}{c_{i-1}+c_i}\right) + \tan\beta_{i-1}$$

$$w_i = -\frac{\Delta l^2}{3}\left(\frac{2\varepsilon_{i-1}+\varepsilon_i}{c_{i-1}+c_i}\right) + \Delta l\tan\beta_{i-1} + w_{i-1}$$

Stepwise Method

Ko et al., 2007

Application remarks

- only strain and neutral axis location are required
- displacement estimate is provided at location of the strain sensor
- accuracy may be reduced due to flawed assumptions

Modal Method

Concept of modal strain

$$\boldsymbol{u}(t) = \begin{bmatrix} \boldsymbol{u}_1(t) \\ \boldsymbol{u}_2(t) \\ \boldsymbol{u}_3(t) \end{bmatrix} \cong \sum_{i=1}^{n} \begin{bmatrix} \phi_{1i} \\ \phi_{2i} \\ \phi_{3i} \end{bmatrix} q_i(t) = \begin{bmatrix} \boldsymbol{\Phi}_1 \\ \boldsymbol{\Phi}_2 \\ \boldsymbol{\Phi}_3 \end{bmatrix} \boldsymbol{q}(t) = \boldsymbol{\Phi}\boldsymbol{q}(t), \quad \boldsymbol{\Phi} \in \mathbb{R}^{3N\times n}$$

$$\boldsymbol{\varepsilon} = \begin{bmatrix} \varepsilon_{11} & \varepsilon_{12} & \varepsilon_{13} \\ & \varepsilon_{22} & \varepsilon_{23} \\ \text{sym.} & & \varepsilon_{33} \end{bmatrix} = \begin{bmatrix} \frac{\partial \boldsymbol{u}_1}{\partial x_1} & \frac{1}{2}\left(\frac{\partial \boldsymbol{u}_1}{\partial x_2} + \frac{\partial \boldsymbol{u}_2}{\partial x_1}\right) & \frac{1}{2}\left(\frac{\partial \boldsymbol{u}_1}{\partial x_3} + \frac{\partial \boldsymbol{u}_3}{\partial x_1}\right) \\ & \frac{\partial \boldsymbol{u}_2}{\partial x_2} & \frac{1}{2}\left(\frac{\partial \boldsymbol{u}_2}{\partial x_3} + \frac{\partial \boldsymbol{u}_3}{\partial x_2}\right) \\ \text{sym.} & & \frac{\partial \boldsymbol{u}_3}{\partial x_3} \end{bmatrix}$$

6 corresponding strain mode shape vectors

$$\longrightarrow \quad \boldsymbol{\varepsilon}_{ij} = \frac{1}{2}\left(\frac{\partial \boldsymbol{u}_i}{\partial x_j} + \frac{\partial \boldsymbol{u}_j}{\partial x_i}\right) \cong \frac{1}{2}\left(\frac{\partial \boldsymbol{\Phi}_i}{\partial x_j} + \frac{\partial \boldsymbol{\Phi}_j}{\partial x_i}\right)\boldsymbol{q} = \boldsymbol{\Psi}_{ij}\boldsymbol{q}, \quad i,j = 1,2,3$$

Modal approach

$$\boldsymbol{u}(t) = \sum_{i=1}^{n} \boldsymbol{\phi}_i q_i(t) = \boldsymbol{\Phi}\boldsymbol{q}(t)$$

$$\boldsymbol{\varepsilon}(t) = \sum_{i=1}^{n} \boldsymbol{\psi}_i q_i(t) = \boldsymbol{\Psi}\boldsymbol{q}(t)$$

independent number, locations, and directions

Modal coordinate estimate

$$\hat{\boldsymbol{q}}(t) = \left(\boldsymbol{\Psi}^T\boldsymbol{\Psi}\right)^{-1}\boldsymbol{\Psi}^T\boldsymbol{\varepsilon}$$

Displacement approximation

$$\hat{\boldsymbol{u}}(t) = \boldsymbol{\Phi}\boldsymbol{\Psi}^{\dagger}\boldsymbol{\varepsilon}$$

DST matrix

Application remarks

- number of strain sensors can be low compared to potential displacement output
- DST matrices can be build from FEM, experiments, and hybrid combination
- normalization of mode shapes required

Internal Strain Instrumentation

LUNA fibre

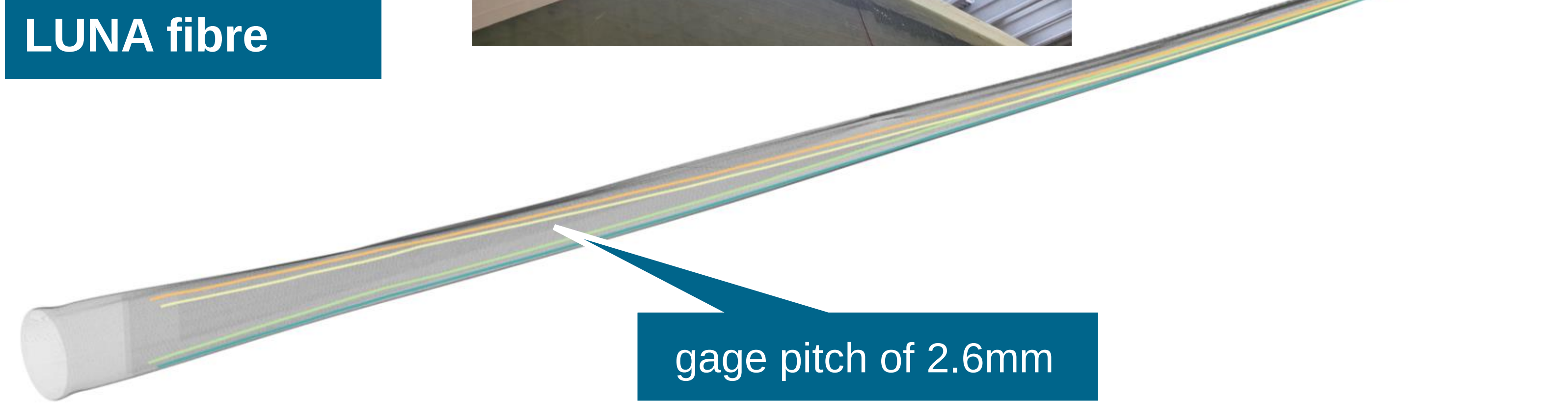

gage pitch of 2.6mm

Used strain sensors

- installation during manufacturing of the blade
- 4 quasi-continuous fibres positioned at shear webs measured with *LUNA ODiSI 6104*
- 128 FBG strain channels distributed on 10 sections measured with *imc CRONOSflex*

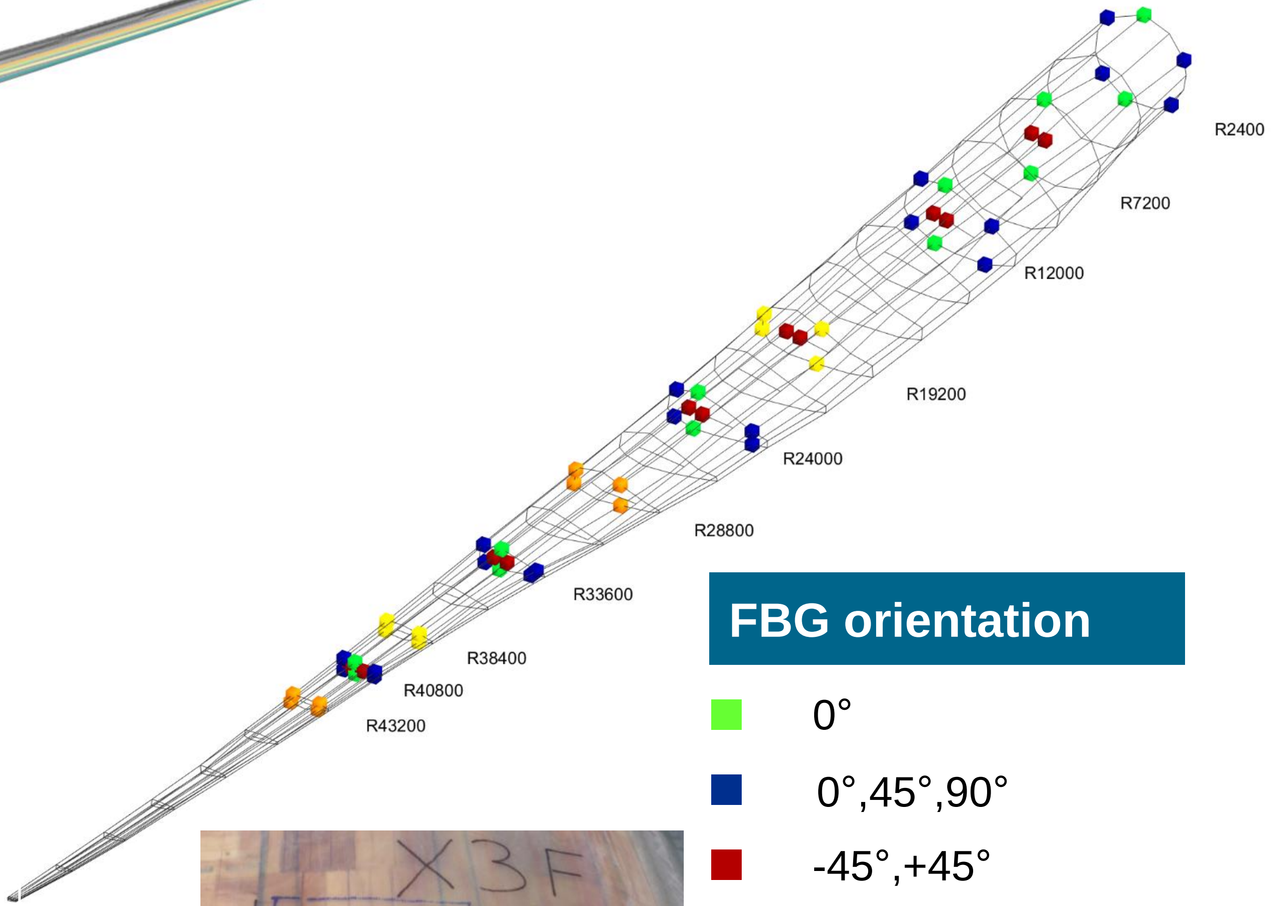

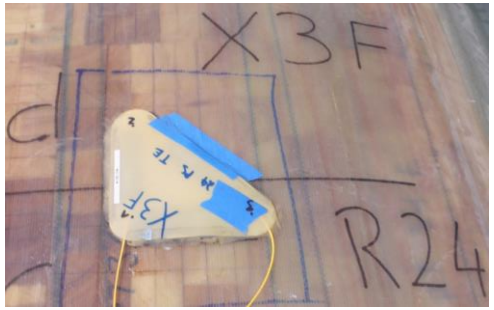

FBG orientation

- 0° (green)
- 0°,45°,90° (blue)
- -45°,+45° (red)
- 0°, 90° (orange)
- 0°, 90°, and temperature (yellow)

Application of Ko‘s method

Strain of MyMinLF5 load case

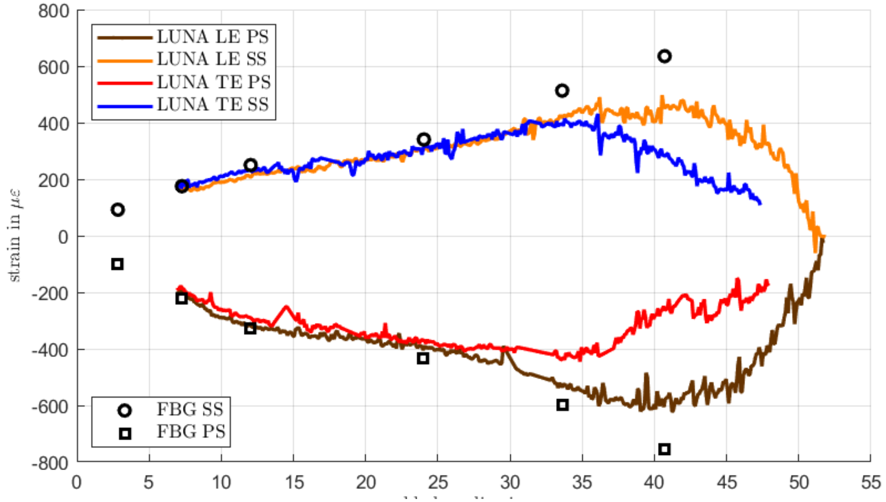

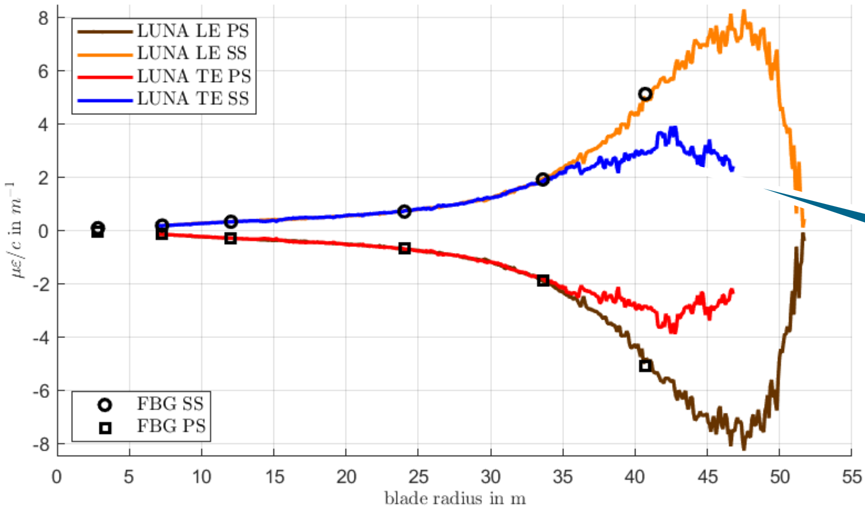

Location of neutral axis

Linear varying strain over thickness:

$$c_i^{ss} = \left(\frac{\varepsilon_i^{ss}}{\varepsilon_i^{ss} - \varepsilon_i^{ps}} \right) h_i$$

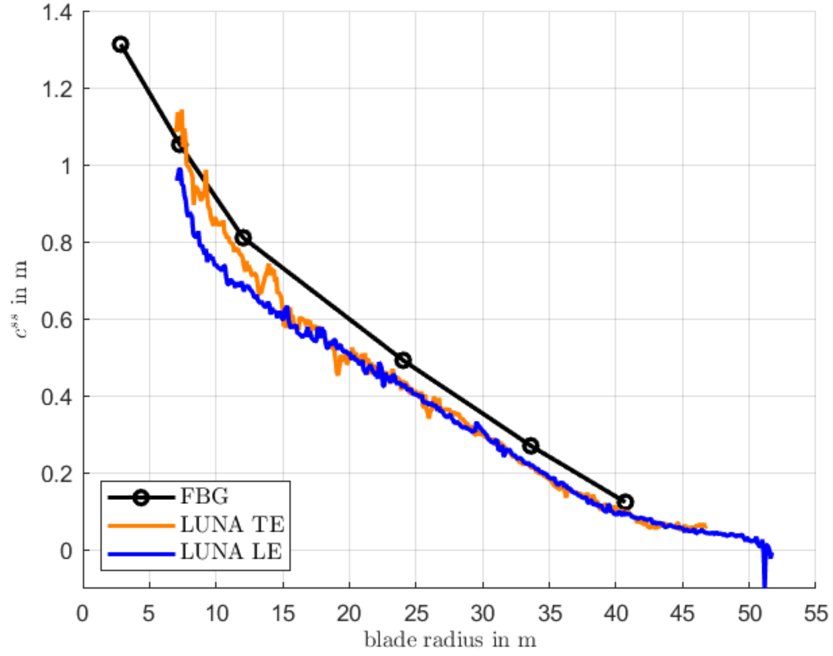

deviation from ideal beam behavior at TE shear web

Modal Testing of the Blade

External accelerometers

- 319 uniaxial IEPE sensors measured with *Simcenter SCADAS Mobile*
- distributed on test rig, blade leading and trailing edge, surface panels, and flange

Modal test setup

- excitation of the structure via electrodynamic long-stroke shaker
  - random and sweep signals
  - different excitation points
  - varying load levels
- determination of FRFs and identification of modal parameters up to 30 Hz
- overall testing time: 7 days

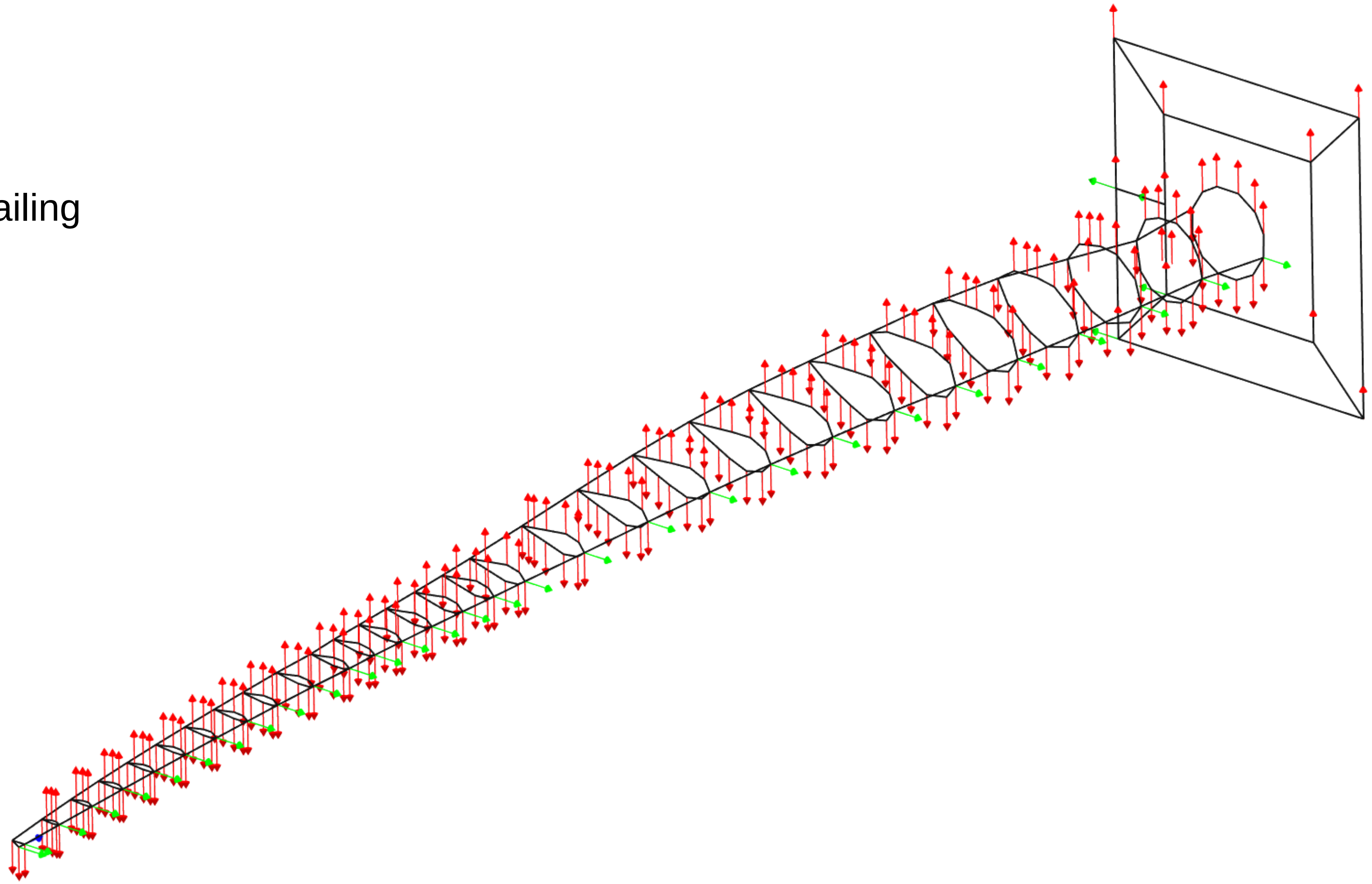

Modal Testing of the Blade

External accelerometers

- 319 uniaxial IEPE sensors measured with *Simcenter SCADAS Mobile*
- distributed on test rig, blade leading and trailing edge, surface panels, and flange

Modal test setup

- excitation of the structure via electrodynamic long-stroke shaker
  - random and sweep signals
  - different excitation points
  - varying load levels
- determination of FRFs and identification of modal parameters up to 30 Hz
- overall testing time: 7 days

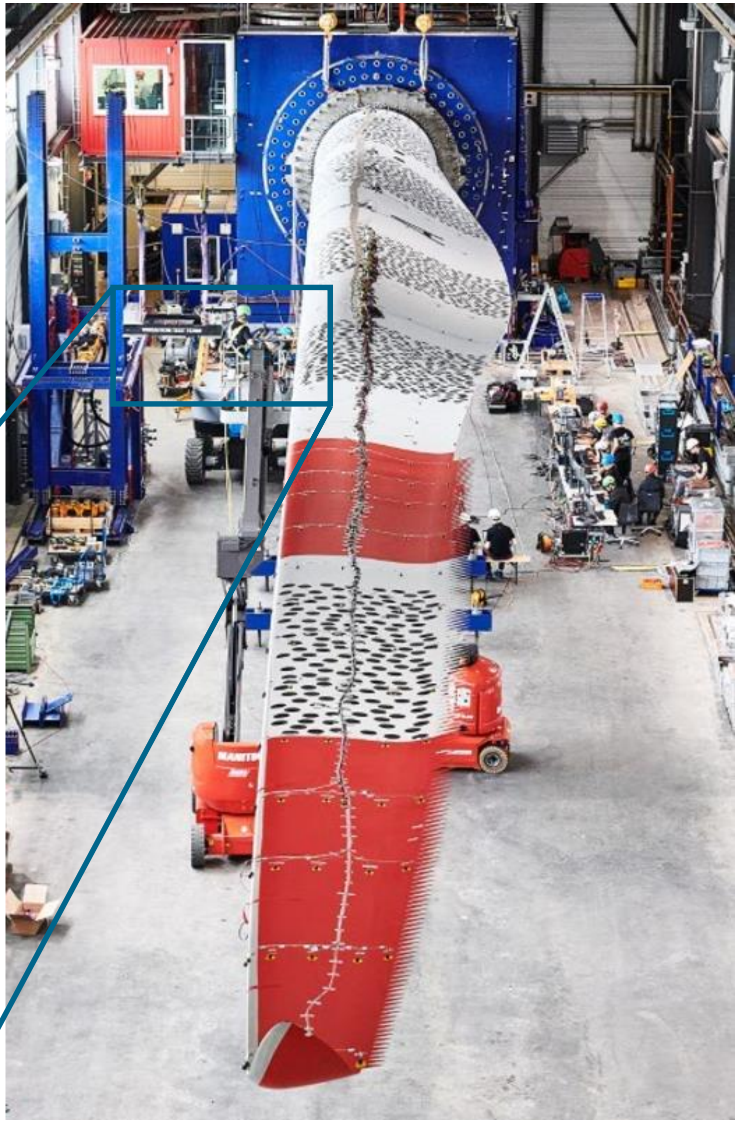

Application of the Modal Method

Time data

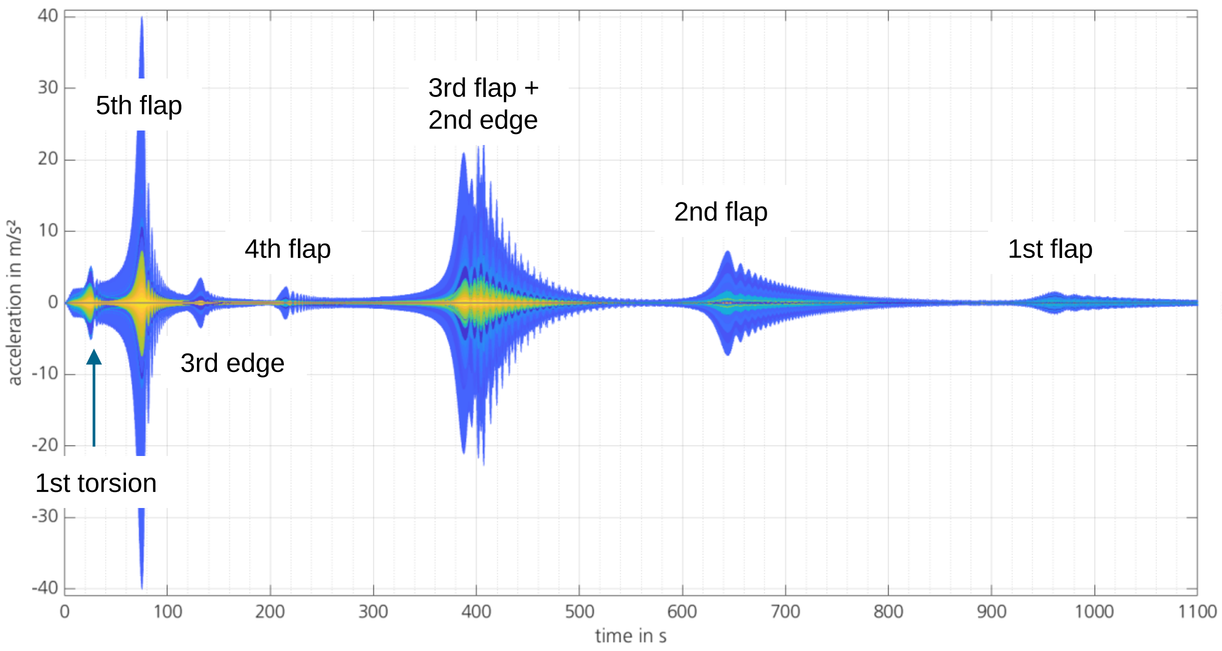

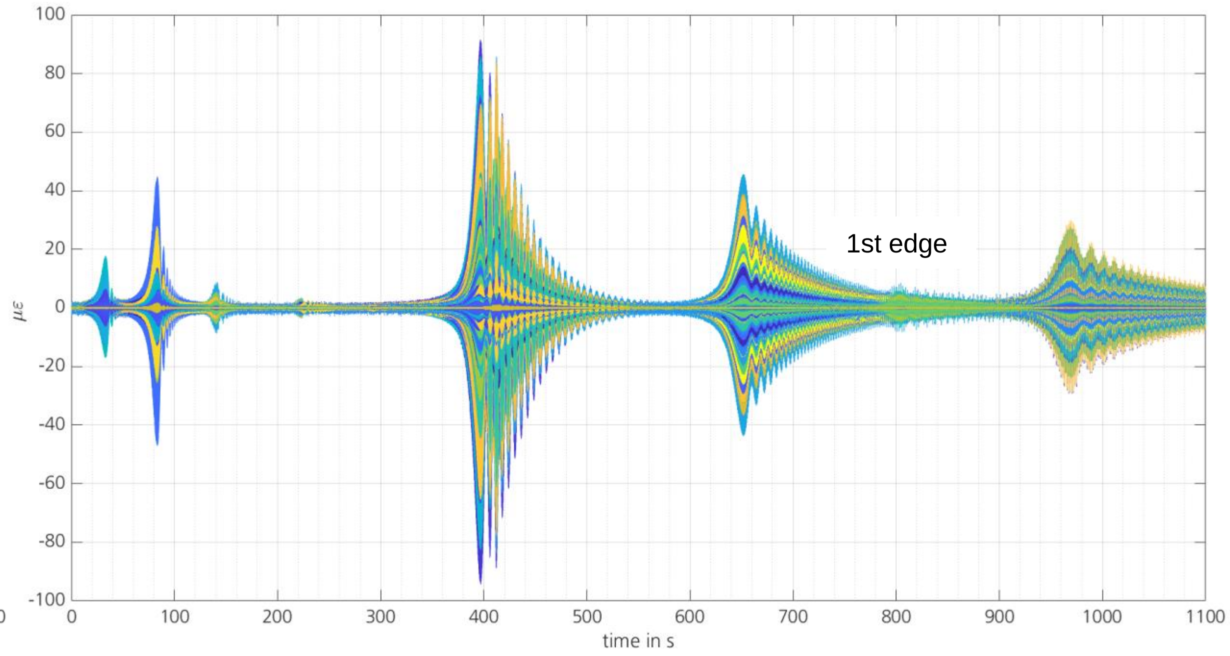

Excitation

- flapwise shaker excitation
- logarithmic down sweep from 10 Hz, 0.25 oct/min
- reduced forces at lower frequencies

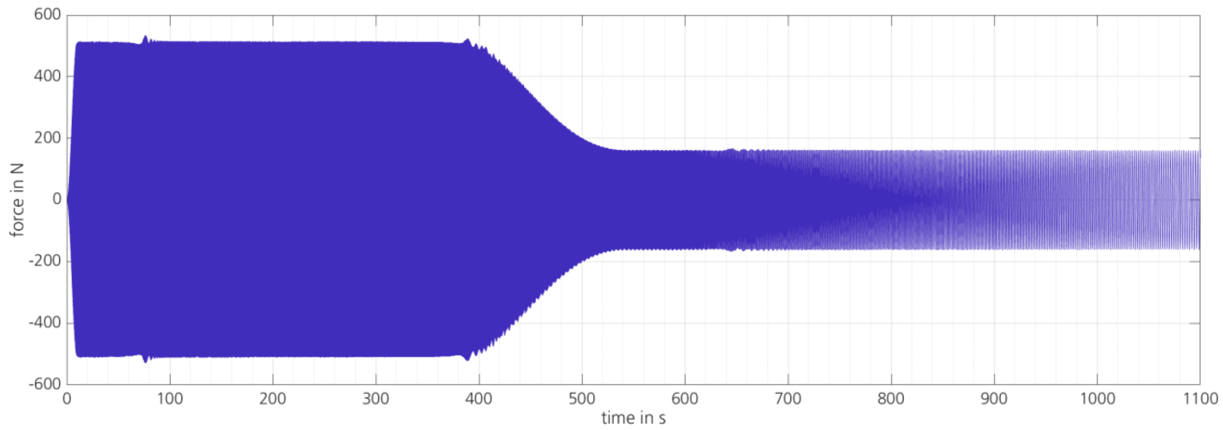

Application of the Modal Method

Frequency response functions

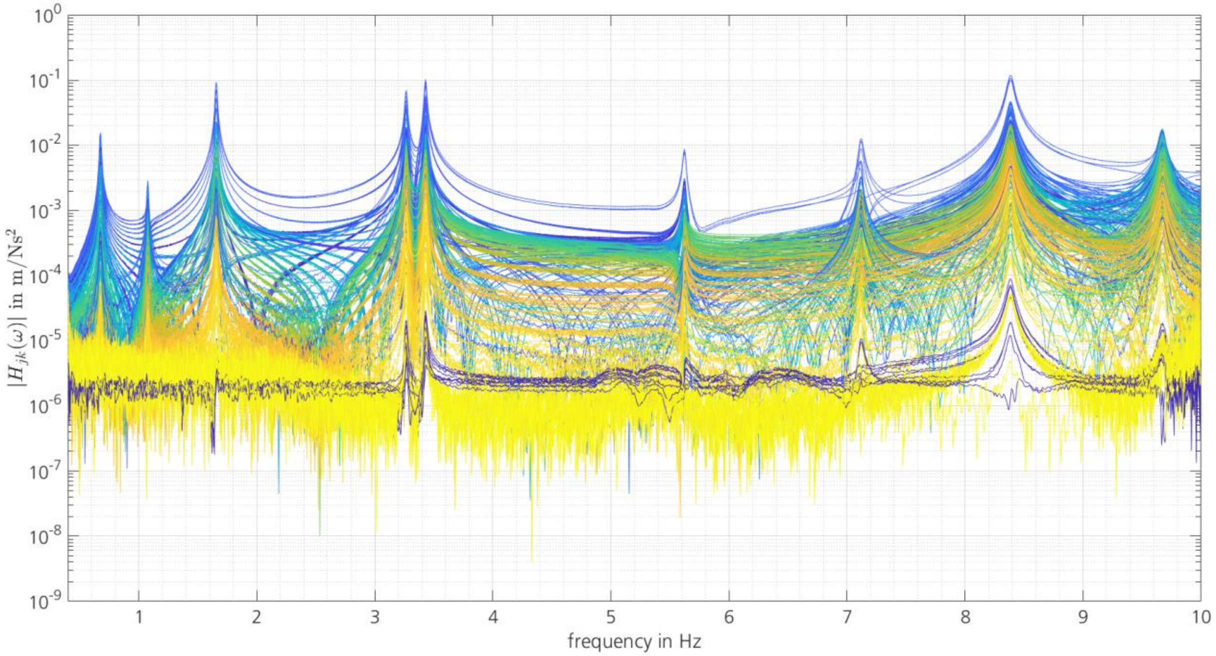

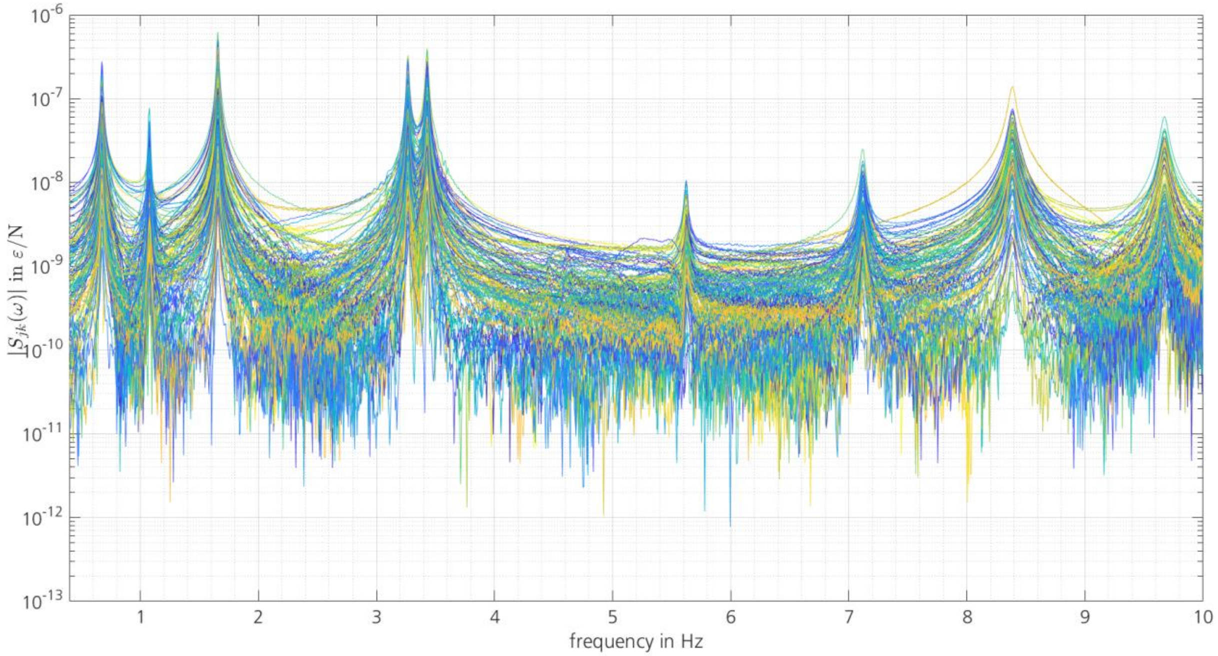

Application of the Modal Method

Mode shapes

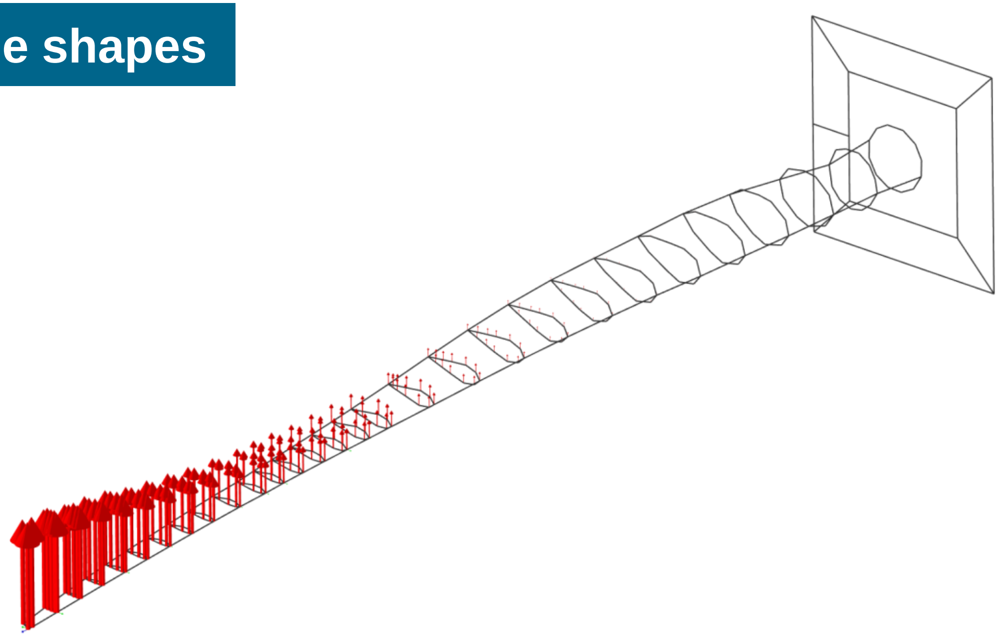

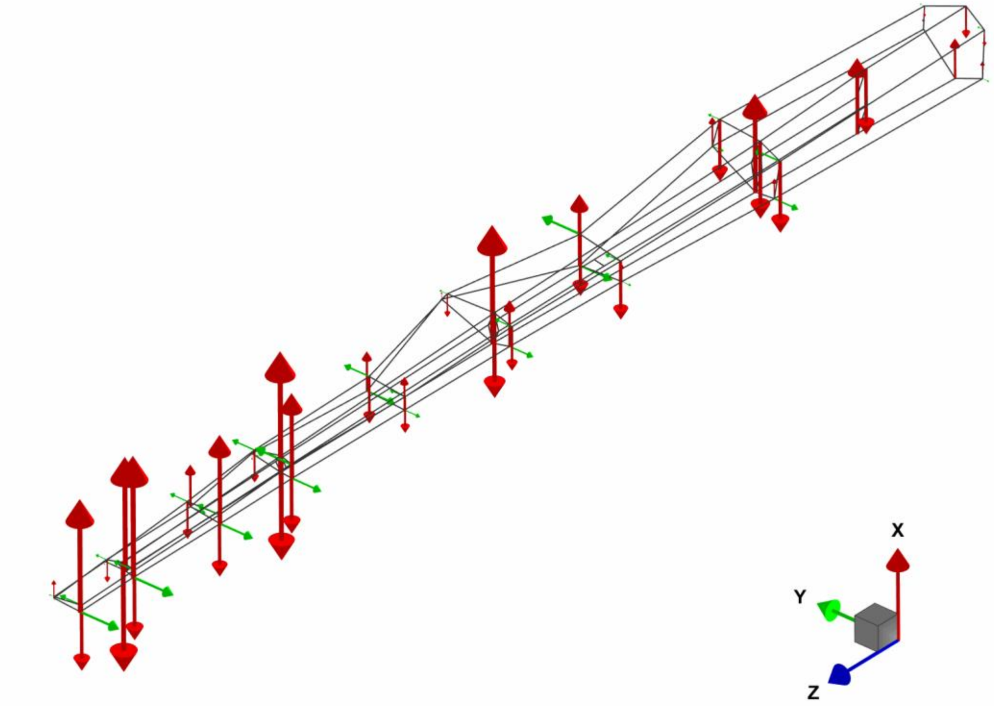

Scaling

$$\overline{H}_{jk}(\omega) = \sum_{r}^{2N} \frac{\overline{r}_{jkr}}{j\omega - \overline{\lambda}_r} \qquad \overline{r}_{jkr} = \frac{\overline{\phi}_{jr}\overline{\phi}_{kr}}{\overline{a}_r} \qquad \xrightarrow[\overline{a}_r = 1]{\overline{H}_{kk}(\omega)} \overline{\phi}_{kr}$$

$$\overline{S}_{jk}(\omega) = \sum_{r}^{2N} \frac{\overline{s}_{jkr}}{j\omega - \overline{\lambda}_r} \qquad \overline{s}_{jkr} = \frac{\overline{\psi}_{jr}\overline{\phi}_{kr}}{\overline{a}_r} \qquad \xrightarrow[\overline{a}_r = 1]{\overline{S}_{jk}(\omega)} \overline{\psi}_{jr} = \frac{\overline{s}_{jkr}}{\overline{\phi}_{kr}}$$

Bernasconi and Ewins, 1989

Properties of modal matrices

- normalization of strain mode shape
- use of real-valued mode shapes
- up to 9 eigenvectors considered

Load case: MyMin LF5

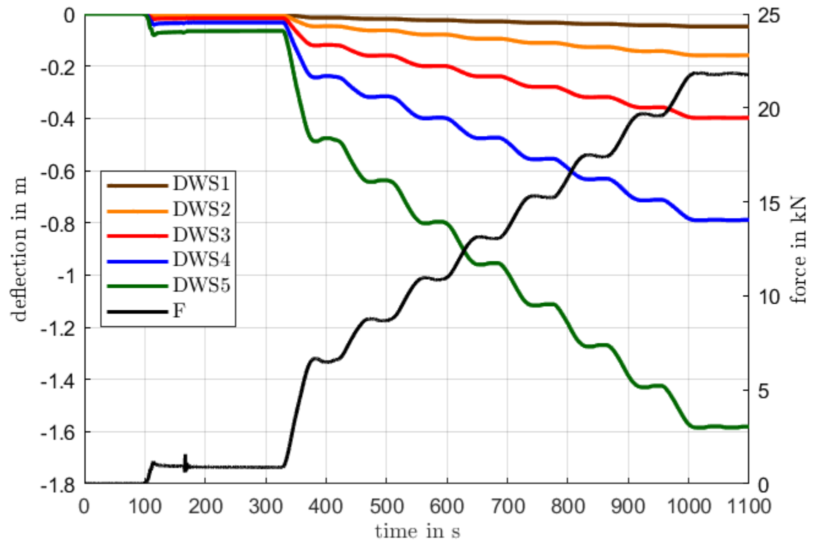

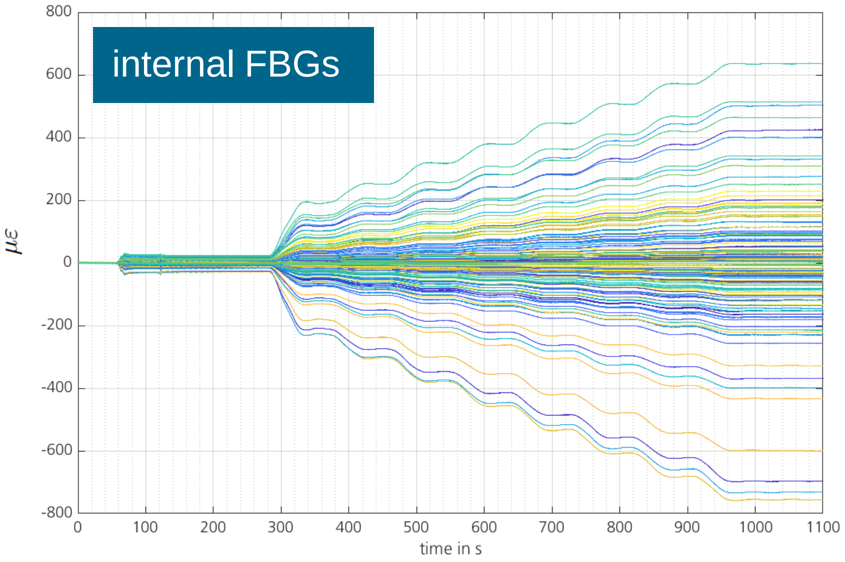

Modal Method displacement reconstruction

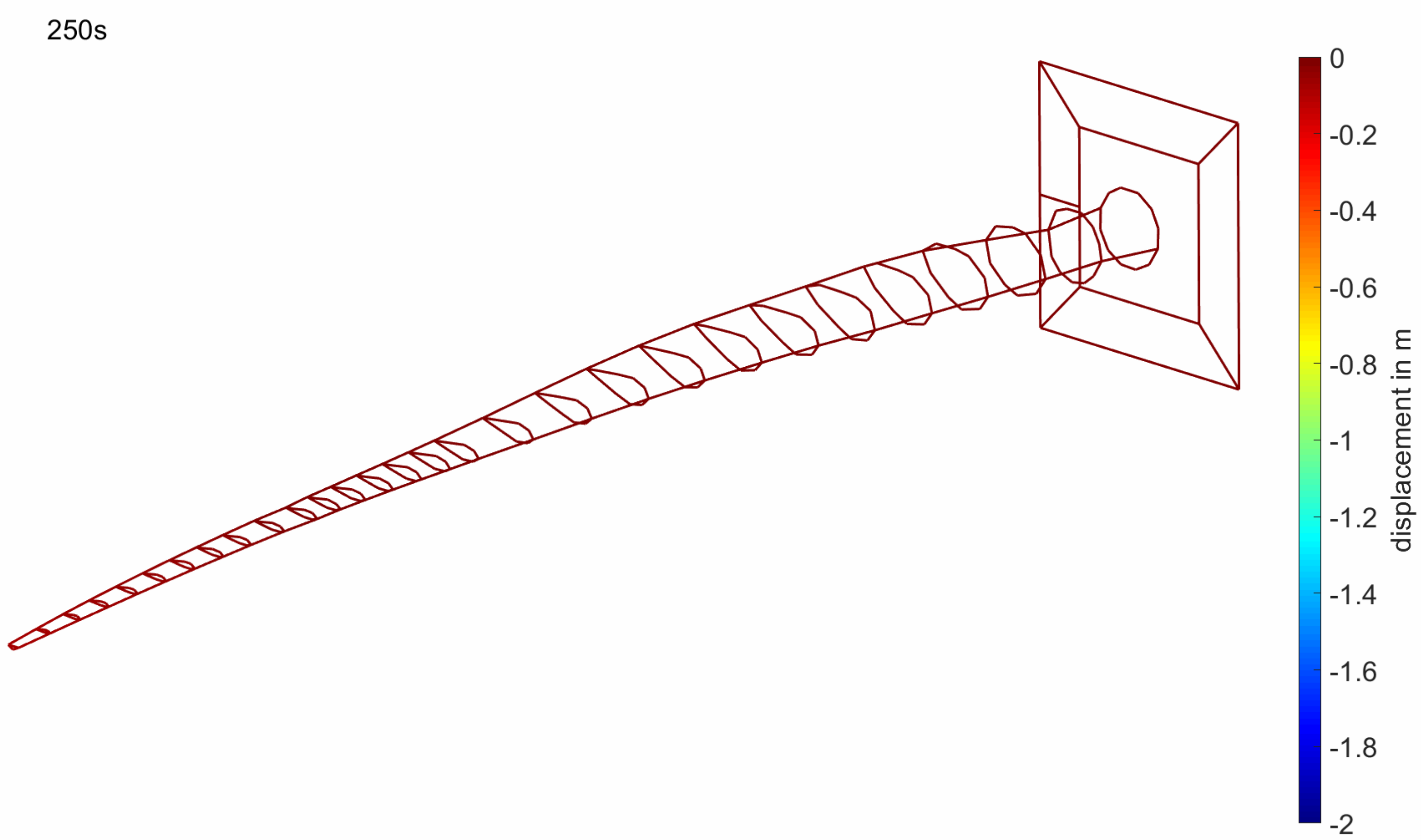

Comparison of Methods

Results overview

- good agreement with all methods applied
- trailing edge strain found inadequate for integration
- Modal Method yields deflection up to blade tip

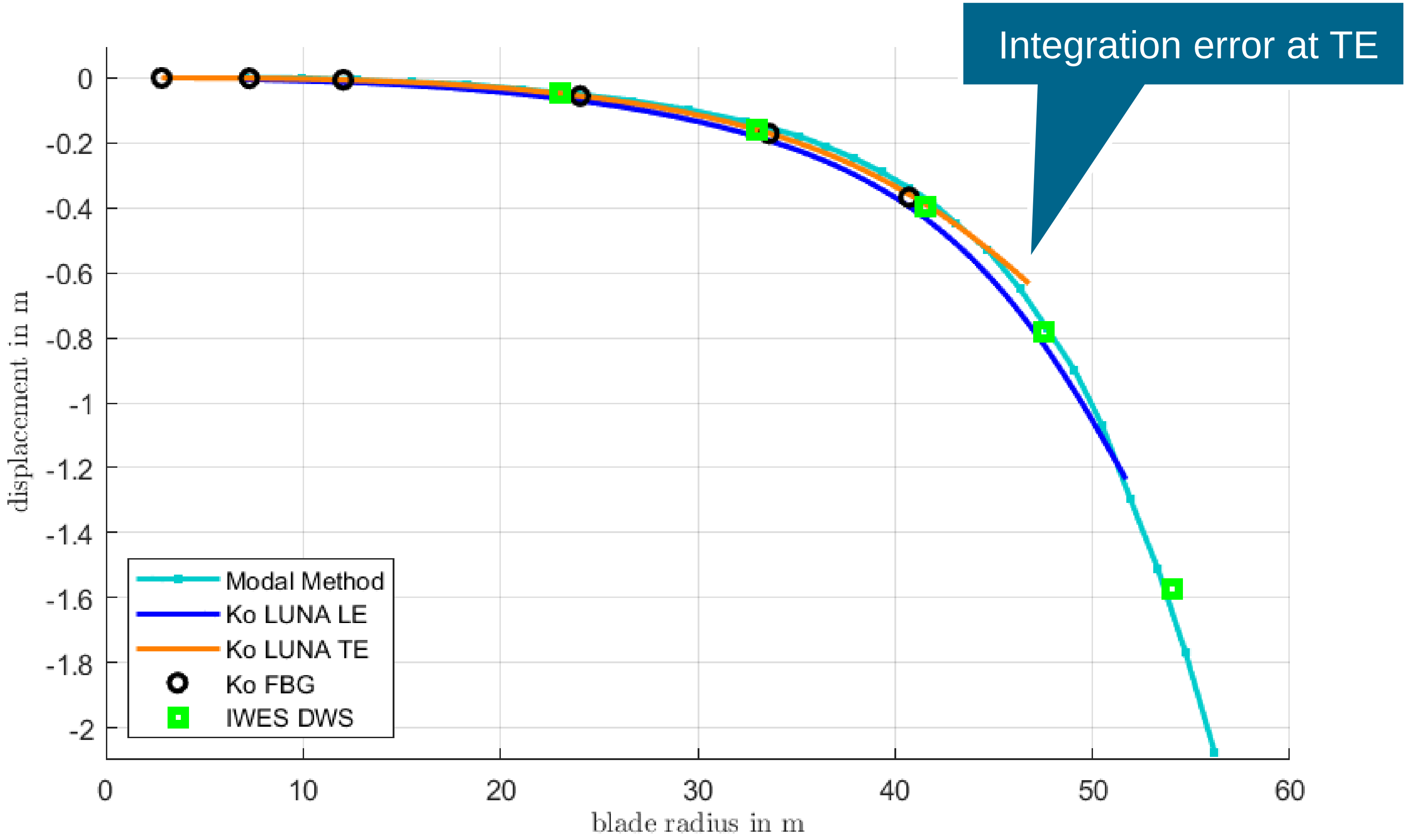

Future Research

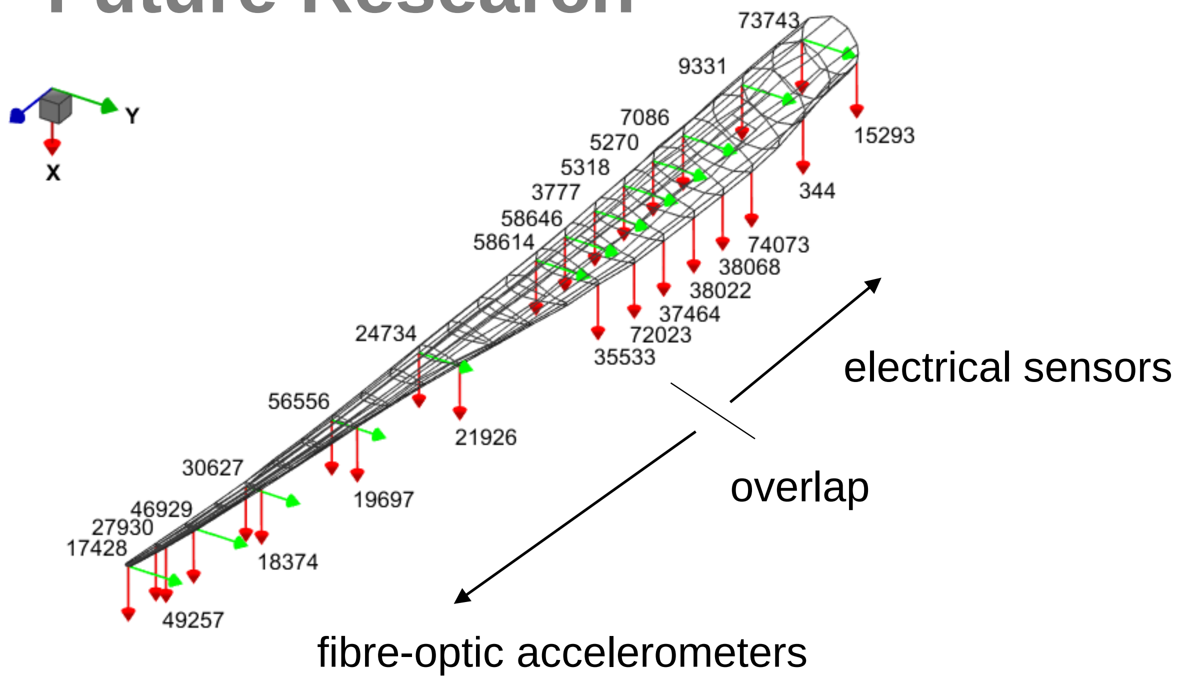

Usage of internal accelerometers

- blades equipped to the tip
- both electric and fibre-optic sensors

Application on real turbine

- different methods for sake of comparison
- deflection and modal parameters monitoring at varying conditions
- several blades simoultaneously

Imprint

Topic: Wind turbine rotor blade deformation reconstruction using shape sensing techniques on quasi-continuous optical fibers and discrete FBGs

Date: 23.05.2023

Author: Janto GUNDLACH, Johannes KNEBUSCH, Yves GOVERS

with help from: Ralf Buchbach, Oliver Hach, Johannes Knebusch, David Meier, Tobias Meier, Jan Schwochow, Julian Sinske, Keith Soal, Martin Tang, Carsten Thiem, Hendrik Verdonck, Robin Volkmar, Martin Gröhlich, Sebastian Zettel, and all members of the DFWind joint research project.

Institute: DLR, Institute of Aeroelasticity

Supported by:

Federal Ministry for Economic Affairs and Climate Action

on the basis of a decision by the German Bundestag